catalysts

MDPI

Article

Copper- and Manganese-Based Bimetallic Layered Double Hydroxides for Catalytic Reduction of Methylene Blue

Muhammad Altaf Nazir [1,*], Aziz ur Rehman [1], Tayyaba Najam [2], Mohamed Farouk Elsadek [3], M. Ajmal Ali [4], Ismail Hossain [5], Muhammad Khurram Tufail [6,*] and Syed Shoaib Ahmad Shah [7,*]

1 Institute of Chemistry, The Islamia University of Bahawalpur, Bahawalpur 63100, Pakistan
2 Institute for Advanced Study, Shenzhen University, Shenzhen 518060, China
3 Department of Biochemistry, College of Science, King Saud University, P.O. Box 2455, Riyadh 11451, Saudi Arabia
4 Department of Botany and Microbiology, College of Science, King Saud University, Riyadh 11451, Saudi Arabia
5 Department of Nuclear and Renewable Energy, Ural Federal University, Yekaterinburg 620002, Russia
6 Centre for Cooperative Research on Alternative Energies (CIC energiGUNE), Basque Research and Technology Alliance (BRTA), Albert Einstein 48, 01510 Vitoria-Gasteiz, Spain
7 Department of Chemistry, School of Natural Sciences, National University of Sciences and Technology, Islamabad 44000, Pakistan
* Correspondence: altaf.nazir@iub.edu.pk (M.A.N.); khurram.ch91@hotmail.com (M.K.T.); shoaib03ahmad@outlook.com (S.S.A.S.)

Abstract: In this study, copper (Cu)- and manganese (Mn)-based layered double hydroxide (LDH) nanosheets were produced by modest and low-cost hydrothermal technique to display an improved photocatalytic performance toward the degradation of aqueous methylene blue (MB). The morphological and structural properties of the as-prepared photocatalysts were characterized through various techniques comprising XRD, FT-IR, SEM, EDS, and their MB degradation activity was evaluated under visible light irradiation. SEM results explore that the synthesized LDH materials have a sheet-like morphology and are stacked layer by layer. Various analysis parameters, such as the effect of the contact time, concentration and pH of MB solutions were performed to optimize the performance of fabricated LDH materials. The results revealed that the as-synthesized CuAl-LDH and MnAl-LDH exhibited a 74.95 and 70.93% removal of MB under solar light within 180 min. Moreover, synthesized photocatalysts showed an excellent performance of up to four regeneration cycles. We believe that this study provides novel mechanistic insights into the design and preparation of highly competent photocatalysts using low-cost materials, with applications in environmental remediation.

Keywords: layered double hydroxide (LDH); photocatalysis; methylene blue; CuAl-LDH; MnAl-LDH; water treatment

check for updates

Citation: Nazir, M.A.; Rehman, A.u.; Najam, T.; Elsadek, M.F.; Ali, M.A.; Hossain, I.; Tufail, M.K.; Shah, S.S.A. Copper- and Manganese-Based Bimetallic Layered Double Hydroxides for Catalytic Reduction of Methylene Blue. *Catalysts* **2024**, *14*, 430. https://doi.org/10.3390/catal14070430

Academic Editor: Anna Kubacka

Received: 30 May 2024
Revised: 25 June 2024
Accepted: 3 July 2024
Published: 5 July 2024

Copyright: © 2024 by the authors. Licensee MDPI, Basel, Switzerland. This article is an open access article distributed under the terms and conditions of the Creative Commons Attribution (CC BY) license (https://creativecommons.org/licenses/by/4.0/).

1. Introduction

Given its importance to global development and health, water is one of the most fundamental elements for humans. The rapid development of the human population is causing a continual increase in the need for water for agricultural activities, industrial activities, and daily living. Actually, water is a necessity for life as we know it on Earth [1,2]. Due to their significant effects on human health and the sustainable development of society, energy depletion and environmental contamination brought on by fast-paced global industrialization have garnered a lot of attention over the past few decades [3]. The aquatic ecosystem and human health are both severely harmed when dye-contaminated effluents are released into aquatic environments [4,5]. Around 70% of all dyes produced worldwide each year are azo dyes, which have an azo group (—N=N—) as the chromophore along with additional functional groups including sulfonic and hydroxyl groups [6]. These

chemicals' natural stability in the presence of light and resistance to microbial degradation make it potentially dangerous to directly discharge them into water courses or to directly discharge their poisonous derivatives into them. A further factor aggravating the issue is the approximately 20% annual dye output lost during the dying process, or over 7×10^5 metric tons [7]. Because it is one of the most widely used compounds in the dye industry, methylene blue (MB) is particularly well-known because it is widely used to color silk, wool, cotton, and paper [8,9]. Therefore, before being disposed of or consumed, it is imperative to develop an effective and environmentally safe process for the breakdown of methylene blue into non-toxic metabolites.

Currently, a number of methods, including adsorption, photocatalysis, advanced oxidation processes, electro-flocculation, membrane filtering, etc., are used to remove these hazardous pollutants from water [10–13]. When it comes to employing renewable solar energy to address challenges of environmental degradation and energy scarcity, photocatalysis is thought to be the most promising technology.

Numerous photocatalytic materials have been thoroughly studied for the removal of water pollution, including ferrites, mesoporous silica, graphene oxide (GO), g-C_3N_4, metal oxide nanoparticles, activated carbons (ACs), layered double hydroxides (LDHs), metal organic frameworks (MOF), etc. [14–19]. Unfortunately, the majority of photocatalysts have drawbacks that restrict their usefulness in the degradation of organic pollutants, such as difficult preparation procedures, absorption restricted to the UV area, and a fast recombination of photogenerated charge carriers [20,21].

Layered double hydroxides (LDHs) are a class of stacked inorganic sheets that are represented by the straightforward formula $M^{2+}M^{3+}$-X, where M^{2+} and M^{3+} stand for the divalent and trivalent metal cations, respectively, inside the hydroxide layer. Owing to its multilayered structure, adjustable acidity–basicity surface, wide range of chemical composition, ion-exchange properties, reactive interlayer space, and ecologically advantageous feature, it is a promising material for a range of applications, including adsorption of pollutants, photocatalysis, electrocatalysis and sensors [22–27]. Furthermore, because of their excellent structural and physicochemical qualities when interacting with contaminants in aqueous solutions, LDHs are fascinating potential catalysts for water treatment [28]. CuAl–CO_3 LDH/BNO_x nanocomposite, for instance, has been reported by Coogan et al. as an efficient way of eliminating rhodamine B, methylene blue, methyl orange, and evans blue [29]. Nazir et al. synthesized ZnAl-LDH and CoAl-LDH to remove methylene blue and methyl orange, respectively [30,31]. Hanifah et al. reported MgAl-LDH for the catalytic degradation of malachite green [32]. ZnFe-CO_3LDH was reported by Dipshikha Bharali et al. using the co-precipitation process, and it was used to degrade phenol and its derivatives under both UV and visible light irradiations [33].

Herein, we reported the facile, easy and economic fabrication technique that is the hydrothermal method for the synthesis of photocatalytic CuAl-LDH and MnAl-LDH materials to degrade methylene blue from aqueous mediums. Furthermore, CuAl-LDH and MnAl-LDH were thoroughly characterized by SEM, EDS, XRD, and FT-IR techniques. In the meantime, MB's photocatalytic performance was studied in a batch procedure using different contact times, initial dye concentrations, and pH values. Additionally, a thorough evaluation of the mechanism, reusability, and photocatalytic degradation kinetics was conducted.

2. Results and Discussion

2.1. Characterization

The morphologies and structures of CuAl-LDH and MnAl-LDH were observed by using a scanning electron microscope (SEM), and the results are shown in Figure 1a,b. Clear lamellar structures on the surface of the CuAl-LDH and MnAl-LDH are presented in the SEM images, which suggested that a hydrotalcite-like catalyst was well prepared via the hydrothermal technique.

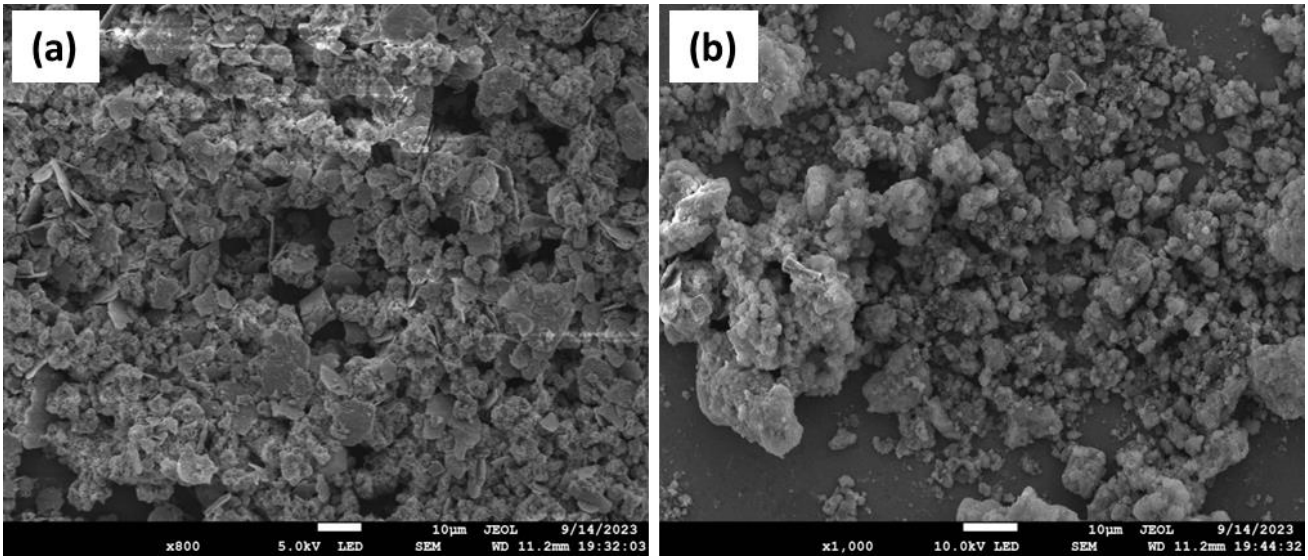

Figure 1. SEM images of (**a**) CuAl-LDH and (**b**) MnAl-LDH.

The experimental molar ratios of copper and aluminum were found to be relatively similar to the planned theoretical stoichiometric values, according to the EDS data. Furthermore, Cu, C, Al, and O as well as Mn C, Al, and O were present in the catalysts CuAl-LDH and MnAl-LDH as they were synthesized, respectively, and no other elements were present. Cu and Mn were found to be uniformly dispersed, indicating homogenously dispersed metal ions, according to the mapping results. The as-prepared MnAl-LDH and CuAl-LDH had an elemental composition of 11% (Figure 2) and 23.2% (Figure 3) of Mn and Cu, respectively. This is satisfactory because the M(II) or M(III) molar ratio x in the range of 0.2–0.33 for the LDH general formula ($[M^{2+}{}_{1-x}M^{3+}{}_{x}\ (OH)_2]^{x+}\ (A^{n-})_{x/n}\ mH_2O$) is generally thought result in LDHs that are more appropriate for a stable structure and composition [34].

The characteristic bands and groups were seen in the as-prepared MnAl-LDH and CuAl-LDH FTIR spectra (Figure 4a,b). The usual metal atomic vibrations that induced the absorption below 1000 cm^{-1} were bands spanning 544 to 954 cm^{-1}, corresponding to Cu-O, Mn-O, or Al-O. These bands contained M-O, M-O-M, and O-M-O bonds [34]. The significant signal with the 1621 cm^{-1} bending mode at 3536 cm^{-1} showed the existence of intercalated OH^-, H_2O [33]. These intercalated structures and abundant metallic bands in CuAl-LDH will provide more reaction sites for the catalytic degradation of methylene blue.

The XRD patterns of MnAl-LDH and CuAl-LDH are displayed in Figure 4c,d. The major peaks recognized for MnAl-LDH are 15.93°, 24.12°, 31.51°, 37.60°, 41.56°, 45.35°, 51.63° and 60.35°. These peaks are attributed to reflection planes of 101, 112, 103, 211, 220, 105, 321, 224 and 400. The successful synthesis of CuAl-LDH was confirmed by the XRD pattern of the as-prepared product, which showed reflections at 2θ angles of 13.62°, 16.38°, 22.68°, 27.98°, 30.88°, 35.95°, 37.70°, 41.24°, and 52.51° (JCPDS 37-0630).

These peaks are related with the main planes 003, 006, 012, 104, 015, 107, 018 and 110. The $Cu(OH)_2$ and Al_2O_3 related peaks that were identified were most likely caused by metal hydroxide breaking down at a high temperature. Sharp peaks indicated a high crystallinity in the CuAl-LDH as synthesized, which was desirable because increased electronic conductivity is a characteristic of high crystallinity [35].

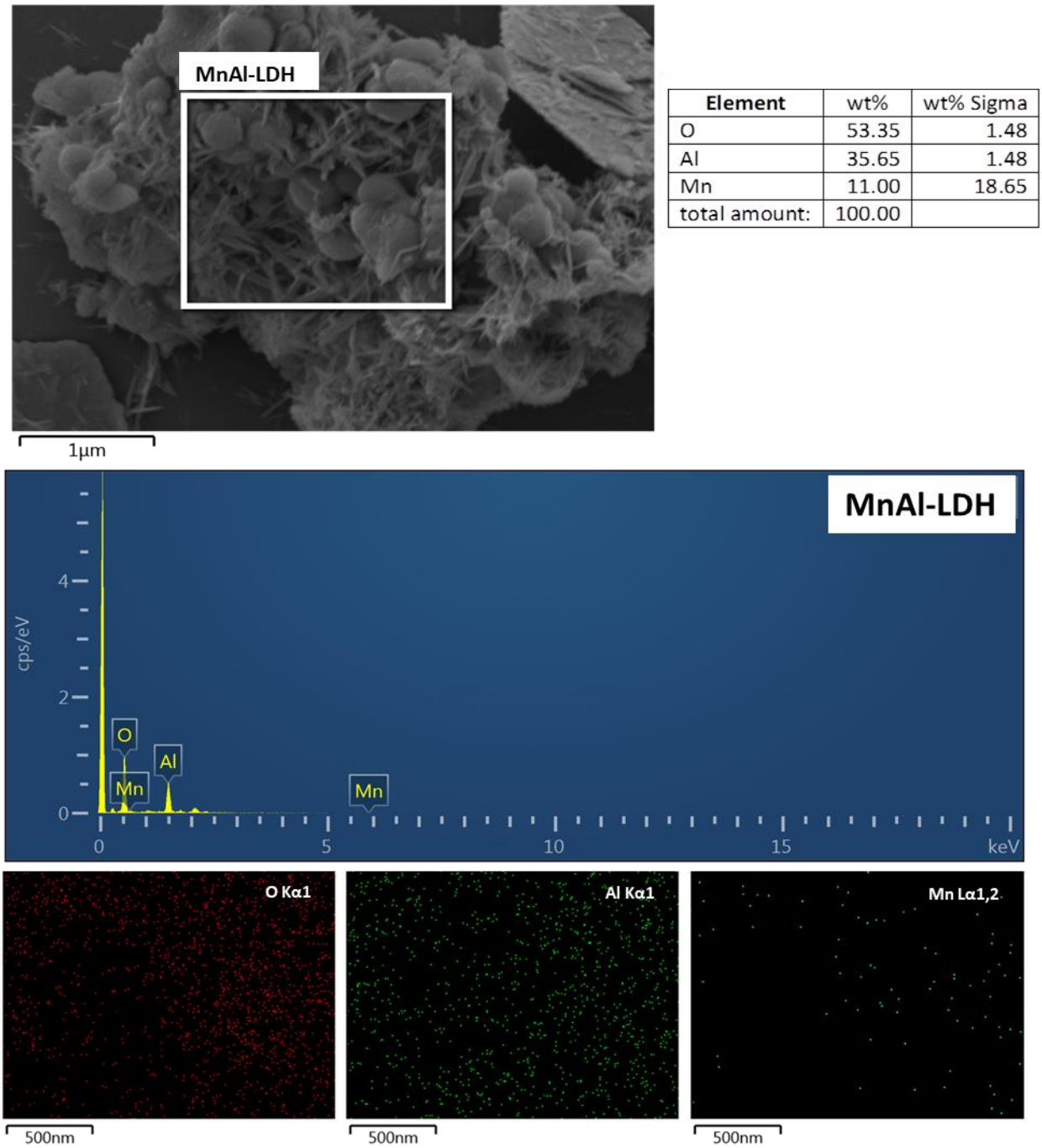

Element	wt%	wt% Sigma
O	53.35	1.48
Al	35.65	1.48
Mn	11.00	18.65
total amount:	100.00	

Figure 2. EDS mapping of MnAl-LDH along with elemental composition.

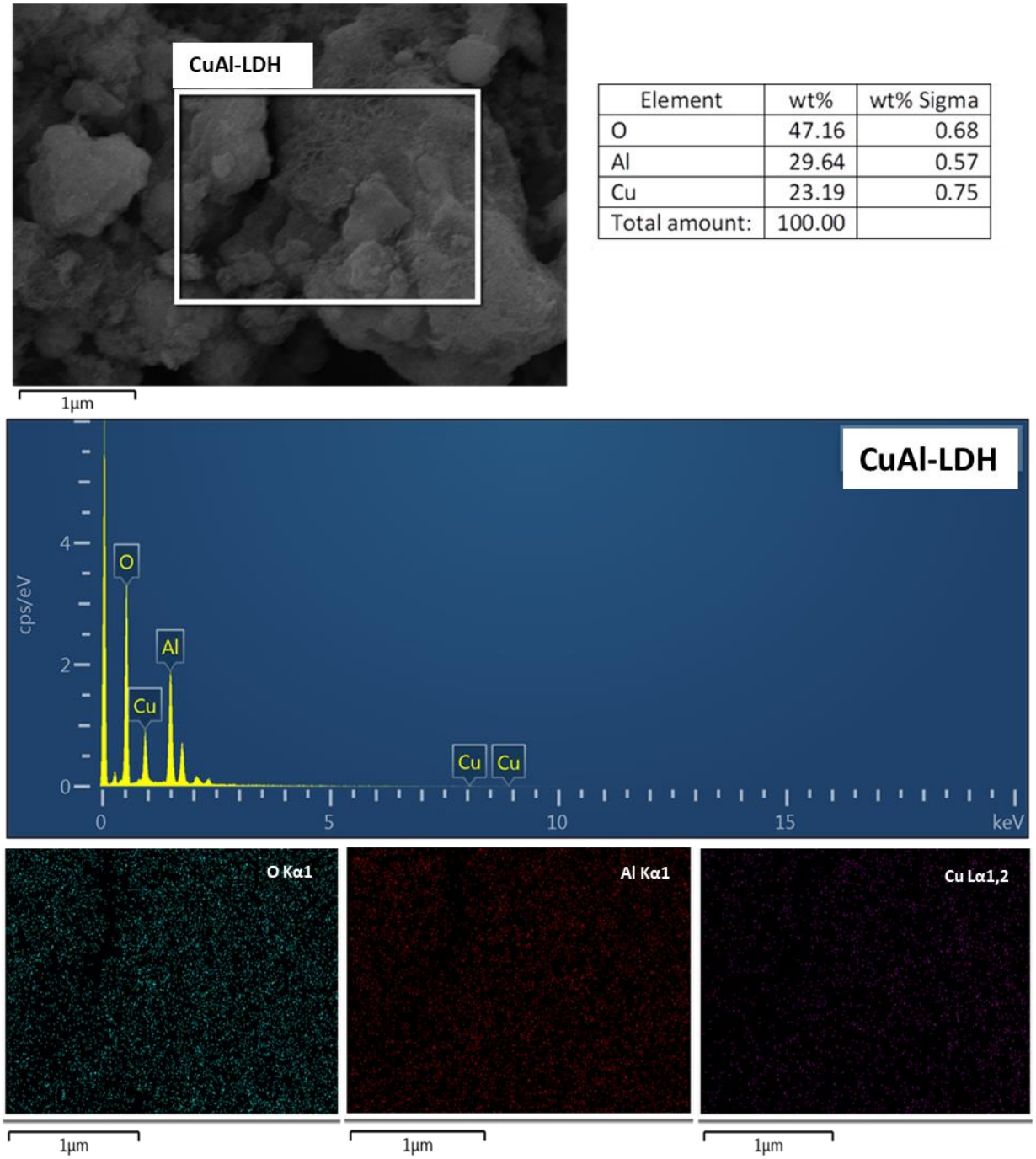

Element	wt%	wt% Sigma
O	47.16	0.68
Al	29.64	0.57
Cu	23.19	0.75
Total amount:	100.00	

Figure 3. EDS mapping of CuAl-LDH along with elemental composition.

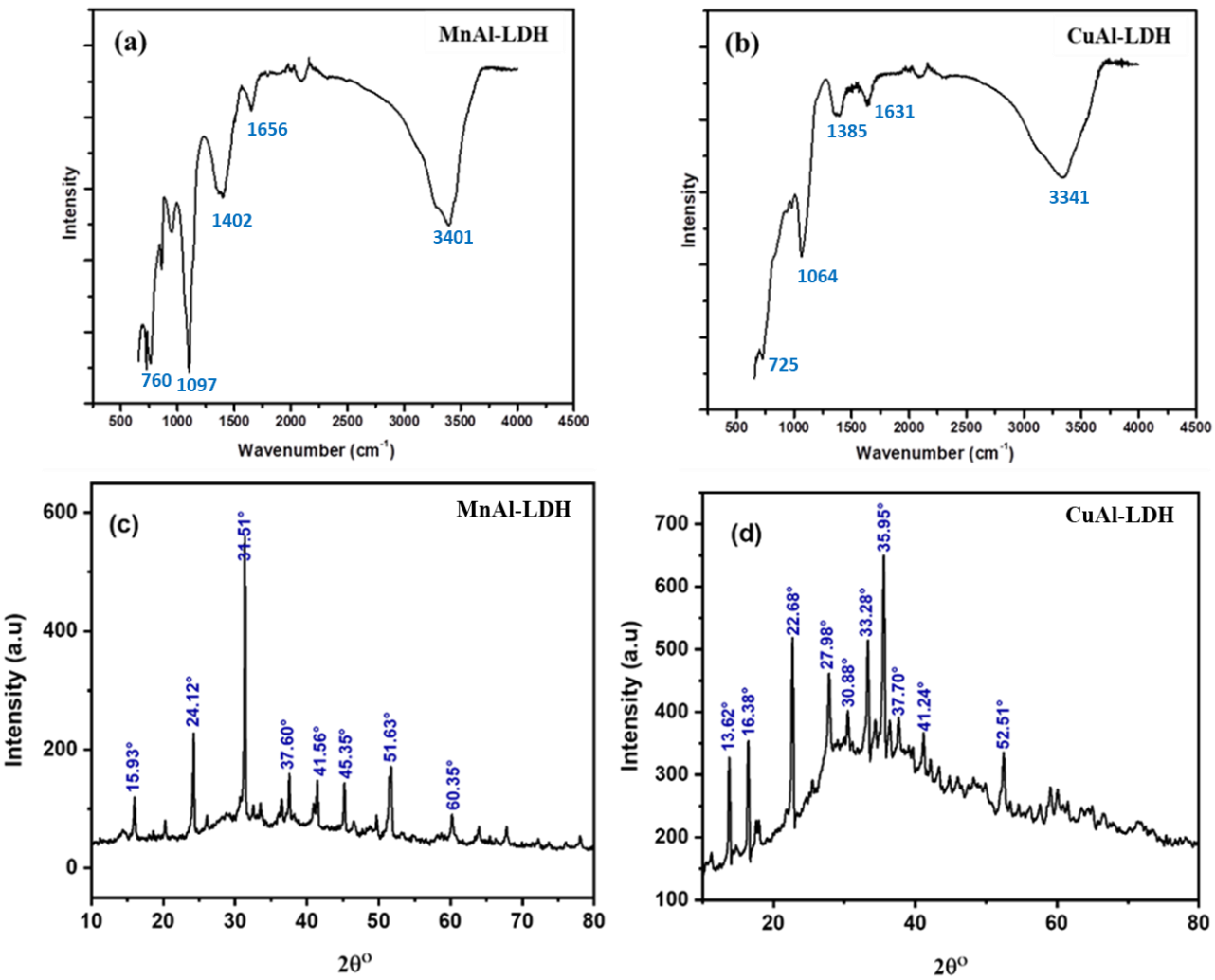

Figure 4. (**a**,**b**) FTIR spectra of MnAl-LDH and CuAl-LDH. (**c**,**d**) XRD spectra of MnAl-LDH and CuAl-LDH.

2.2. Photocatalytic Study

The photocatalytic activity of the obtained CuAl-LDH and MnAl-LDH nanosheets was studied for the degradation in visible light irradiation of MB as a model organic contaminant. A total of 0.02 g of each LDH catalyst was used for the degradation of a 20 mL solution of MB having a concentration of 20 mg/L. The reaction mixture was continuously stirred while being maintained in the dark at room temperature for 30 min in order to assess the synthesized photocatalysts' adsorption capabilities. Subsequently, the reaction mixture was exposed to visible light, and a spectrophotometer was used to determine the degree of deterioration. When synthesized photocatalysts were exposed to a certain wavelength of light, the valence electrons moved from a lower energy state (the valence band or oxidation area) to a higher energy state (the conduction band or reduction region), resulting in the production of e^-/h^+ (electron/hole). As reported, the band gap of CuAl-LDH was 3.70 eV [36]. This narrow band gap was quite essential for the catalytic reduction of pollutants. The results exposed that after 180 min of contact time, 74.95 and 70.93% MB was degraded with CuAl-LDH and MnAl-LDH nanosheets, respectively (Figure 5a–d). These degradation results of CuAl-LDH and MnAl-LDH were comparable with the reported literature (Table 1). CuAl- and MnAl-LDH nanosheets had a better activity because of their well-defined pore sizes, smooth and functionalized surface morphology, more crystalline phase, and excellent photoinduced charge transportation (e^-/h^+ pair

charge). These characteristics also lessen the tendency of e^-/h^+ pair recombination to produce side products, which aids in the facilitation of oxidation-reduction events.

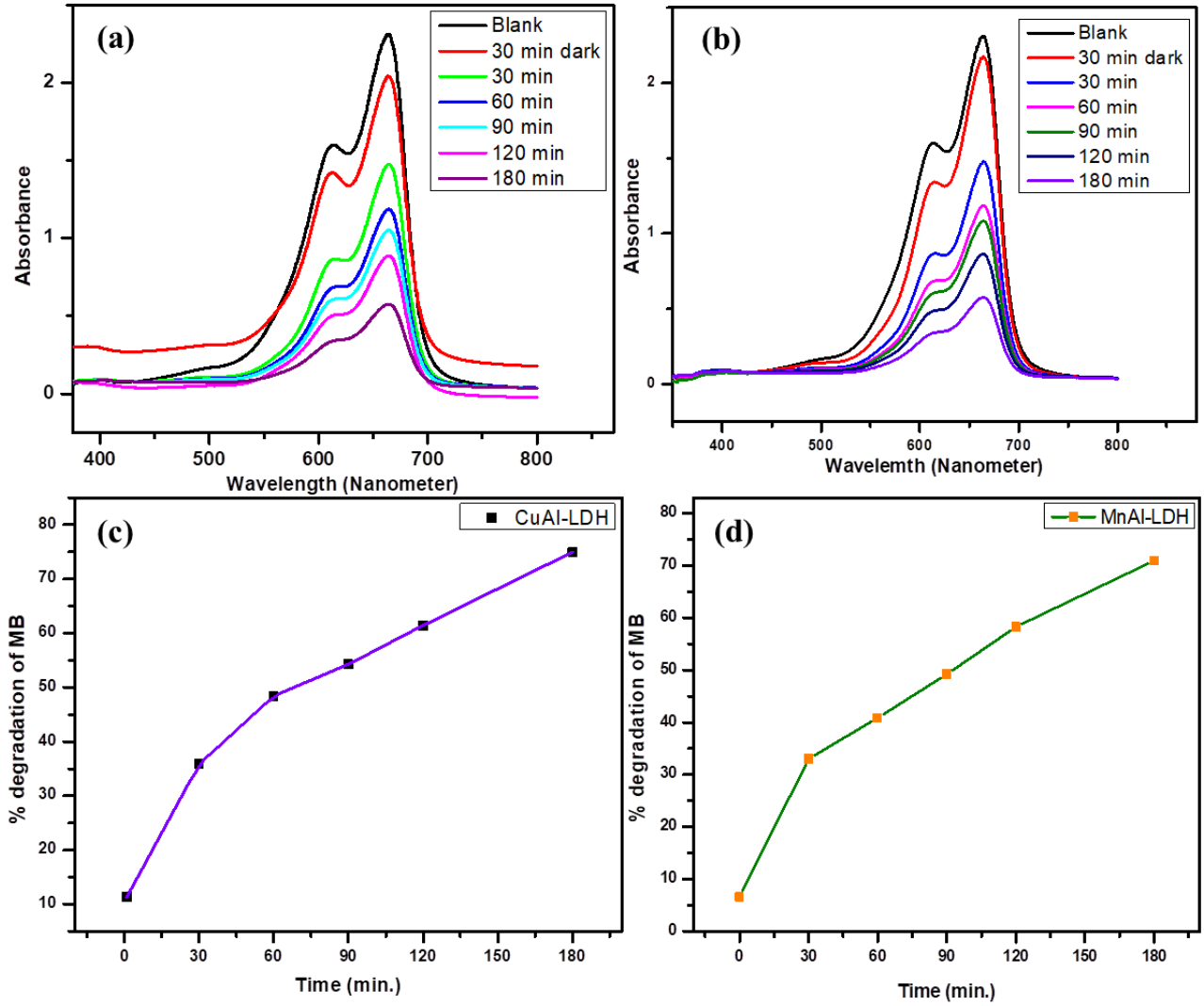

Figure 5. (**a**,**c**) Degradation of MB with CuAl-LDH with respect to time; (**b**,**d**) degradation of MB with MnAl-LDH with respect to time.

2.3. Effect of pH of MB Solution

Figure 6a,b illustrate how the pH factor, which is important in enhancing the degradation performance of synthetic materials, works. The dye's adsorption on the photocatalyst surface, the mode of charge transfer, the dye's properties, and the reactants and products involved in photocatalysis are all significantly impacted by pH [37]. NaOH and HCl were used to change the pH in order to improve the photocatalytic performance. The results exposed that CuAl-LDH and MnAl-LDH give a good performance in basic medium compared to acidic or neutral mediums. The pace of degradation is slowed down by MB because it is less adsorbed and electrically repelled from the surface of LDHs, since both of them take up positive surface charges at a lower pH (pH = 3). Similarly, higher pH inhibits the static interaction between LDH nanosheets and MB due to the massive formation of OH^- under an alkaline medium, making it challenging to promote superior MB decomposition. This is because an alkaline medium (pH greater than 10) causes significant OH^- production [38]. Furthermore, the pace of degradation may be slowed down if the oxygen-containing functional groups of the LDH nanosheets dissolve in a more acidic or alkaline medium.

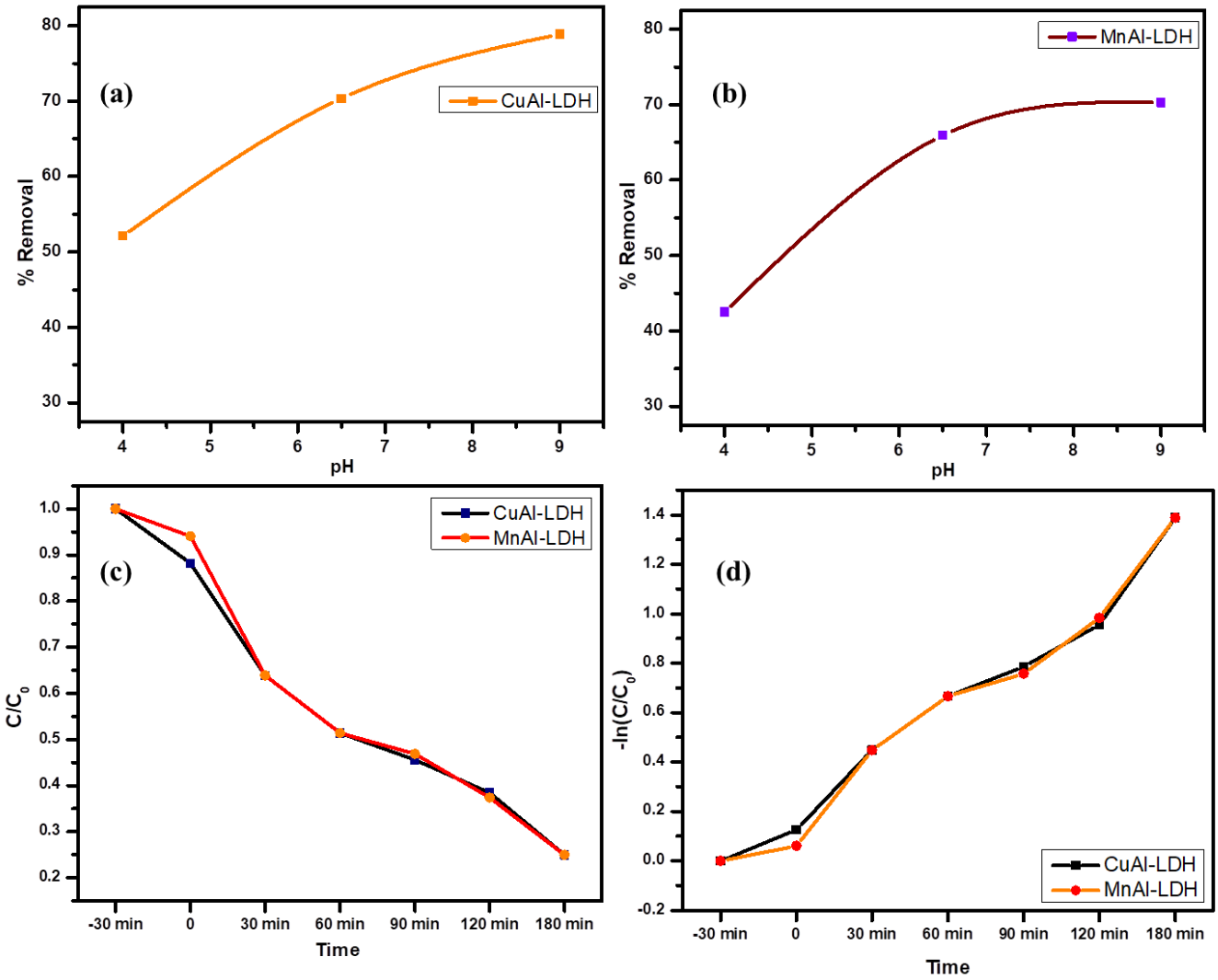

Figure 6. (**a**,**b**) Effect of pH of MB on catalytic performance of CuAl-LDH and MnAl-LDH. (**c**,**d**) Kinetic study of degradation of methylene blue with CuAl-LDH and MnAl-LDH.

2.4. Effect of Initial Concentration of MB

A critical factor in increasing the photocatalytic degradation activity is the dye concentration. A dye concentration increase of 05–25 ppm greatly accelerated the pace of degradation. This is a result of more •OH forming on the photocatalyst surface and combining with the MB dye to produce the final dye degradation (CO_2 + H_2O). It was made abundantly evident that the time needed to attain equilibrium was not much impacted by initially applied concentrations of MB and that the removal ratios improved as the initial concentrations decreased [39].

2.5. Kinetics Studies

The degradation performance of created photocatalysts can be expressed using the Langmuir–Hinshelwood equation, which can be used to find the rate of photocatalytic degradation, as seen below [40]:

$$dC/dt = -k_1 C \quad (1)$$

$$\ln (C/C_0) = k_1 t \quad (2)$$

where k_1 (1/min) is the first-order rate constant, and C/C_0 is the ratio of the initial and time-varying dye concentrations of methylene blue.

The concentrations of MB in solution at time t and the starting concentrations of MB, represented by C_0 and C_t, respectively, yield the apparent first-order rate constant, represented by the value of k or slope. As is shown in Figure 6d, pseudo-first-order kinetics best fit the degradation of MB on CuAl-LDH and MnAl-LDH, with R^2 values of 0.987 and 0.978 for CuAl-LDH and MnAl-LDH, respectively. The rate constants for CuAl-LDH and MnAl-LDH calculated by linear fitting were 0.00663 min^{-1} and 0.00679 min^{-1}, respectively.

Using the equation, the MB degradation rate values for CuAl-LDH and MnAl-LDH are 0.00663 min^{-1} and 0.00679 min^{-1}, respectively. The results show that, as compared to CuAl-LDH, the pseudo-first-order rate constant increases and has a superior degradation efficiency with MnAl-LDH.

Table 1. Comparison of degradation efficiency of CuAl-LDH and MnAl-LDH for the removal of MB with the reported literature.

Catalyst	Reaction Parameters	% Degradation	Ref.
CuAl-LDH	180 min, visible light	74.95	Current study
MnAl-LDH	180 min, visible light	70.93	Current study
$Ca_{0.5}Pb_{0.5-x}Yb_xZn_yFe_{12-y}O_{19}$ hexaferrite	90 min, visible light	96.1	[41]
g-C_3N_4/ZnO-W/$Co_{0.010}$ composite	90 min, visible light	90	[42]
Zn-PMOS	60 min, Tungsten bulb (200 W)	48	[43]
ZnO	90 min, visible light	88	[44]
ZIF-67@wood	--	90	[45]
CMO/CFO/PMS	30 min,	99	[46]
Biosynthesized ZnO	240 min, UV-light	80	[47]
MoS_2/TiO_2	120 min, visible light	98.5	[48]
$ZnS/Zn(CO_3)_2(OH)_6$	80 min, sunlight	56	[49]
TiO_2-decorated CNTs	180 min, visible light	85	[50]

2.6. Proposed Degradation Mechanism

There are various characterization methods used to confirm the composition, characteristics, and photocatalytic activity of CuAl- and MnAl-LDH nanosheets towards MB degradation. In this sense, we predicted the mechanism leading to the MB degradation route's appearance. Figure 7 shows the diagrammatic depiction of the mechanistic approach. It is commonly known that photogenerated active radicals, including electrons, holes, and reactive oxygen species (ROS), are essential to the deterioration of organic dyes.

Below is a summary of the many processes that the dyes go through as they degrade.

$$\text{CuAl-LDH/MnAl-LDH} + h\nu \rightarrow h^+ + e^- \quad (3)$$

$$OH^- + h^+ \rightarrow {}^{\bullet}OH \quad (4)$$

$$2H_2O + h^+ \rightarrow 2{}^{\bullet}OH + 2H^+ \quad (5)$$

$$MB + \cdot OH \rightarrow \text{Degraded products} \quad (6)$$

CuAl-LDH's band gap of 2.12 eV [51] is modest enough to make it simple to excite the catalyst with visible light. The small band gap may lower the energy required for the electron–hole transition between the valence and conduction bands [52]. Its strong photocatalytic activity may also be explained by additional elements, including the photocatalysts' high specific surface area and extremely crystalline structures [53]. The great adsorption capacity that highly crystalline structures and a high specific surface area would provide to the target molecules would facilitate the production of photo-induced electron–hole pairs of active sites.

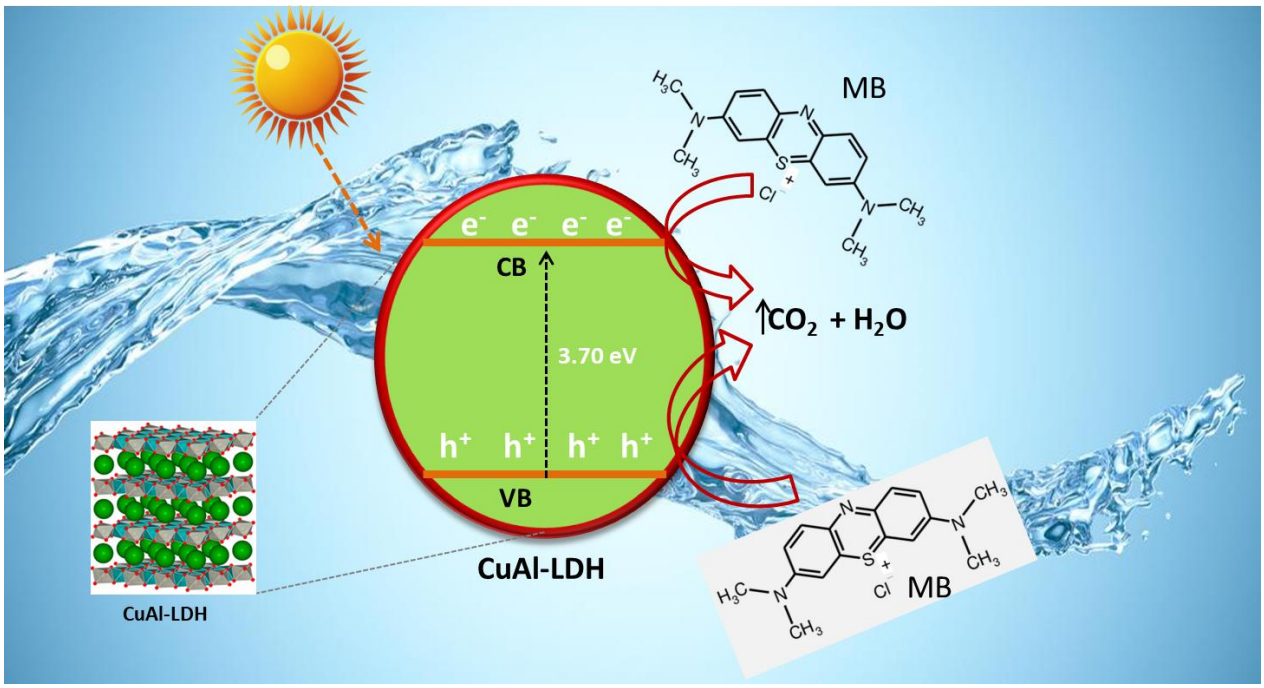

Figure 7. Photocatalytic reduction mechanism of methylene blue over MnAl-LDH/CuAl-LDH.

2.7. Quenching Active Species Trapping Experiment

To leverage the active species trapping assay, reactive species involved in the breakdown of the MB dye were further investigated. Some radical or reactive species may play a pertinent role in the degradation of dyes, including holes (h^+), hydroxyl ($OH^\bullet$), and superoxide radicals ($O_2^{\bullet-}$). To furnish a result, 1 mL of 0.5 mM aqueous solution of ethylenediaminetetraacetic acid (EDTA), isopropyl alcohol (IPA), and para benzoquinone (p-BQ) were added individually to the dye solution. The degradation process of dyes was conducted under conditions similar to those discussed earlier for the degradation of MB dye. The study included investigating the quenching effect of various scavengers and evaluating the efficiency of CuAl-LDH in degrading MB. In the absence of scavengers, the CuAl-LDH degradation efficiency was 70.93%. The degradation efficiency dropped to 33% and 31%, respectively, in the presence of EDTA and IPA. On the other hand, the MB degradation efficiency decreased to merely 68%, respectively, upon adding BQ to the MB dye solution. From the outcome, it is believed that the main species causing MB degradation are h^+ and $OH^\bullet$ radicals. Furthermore, it is concluded that e^- and $O_2^{\bullet-}$ species degrade smaller amounts of MB. Figure 8c illustrates the effect of various radicals on the MB dye degradation process.

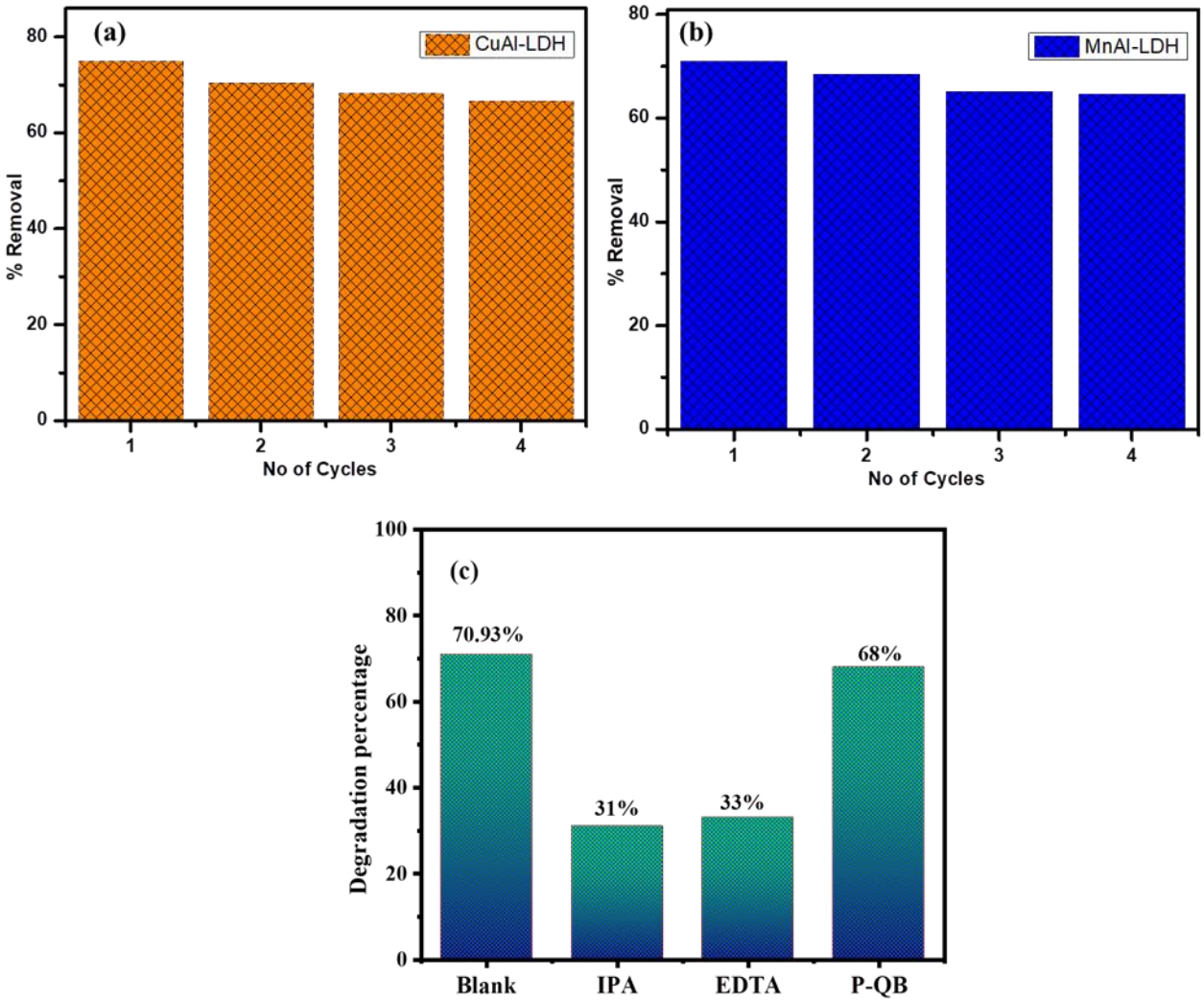

Figure 8. (**a**) Reusability test of CuAl-LDH for the removal of MB. (**b**) Reusability test of MnAl-LDH for the removal of MB. (**c**) Quenching of active radical test.

2.8. Reusability Test

In the current study, the reusability of produced photocatalysts, CuAl-LDH and MnAl-LDH nanosheets, was investigated under optimal reaction conditions (photocatalyst weight of 0.02 g, dye concentration 20 ppm, reaction duration 180 min) using four consecutive reaction cycles. Prior to running the subsequent cycle, the catalyst powder was dried at 60–100 °C for one hour after each run or cycle and cleaned with distilled water. The degradation efficiency of CuAl-LDH in its fourth run was 66.7%, which was an 11% decrease as compared to the fresh/unused CuAl-LDH catalyst. Similarly, MnAl-LDH degraded by 64.7% in its 4th cycle, which was a decrease of under 9% compared to the fresh/unused catalyst (Figure 8a,b).

After undergoing four cycles, the photocatalyst's cyclic stability and structural integrity were found to be over 90%. To eliminate any organic contaminants or dust particles, the photocatalyst was vacuum-filtered using Whatman filter paper and rinsed twice with deionized water. However, it was observed critically that the following factors may contribute to a decrease in degradation efficiency: (i) The photocatalyst's decreased number of surface functional groups as a result of the high moisture content; (ii) Weight loss of the catalyst throughout the process of reuse in a series of cycles; (iii) The effectiveness of degradation in each cycle may be influenced by the presence of organic contaminants or excessive O_2 production during the reaction process.

3. Experimental Section

3.1. Materials

Sigma Aldrich (Devon, UK) supplied the copper nitrate (>98%), aluminium nitrate nonahydrate (>98%), manganese nitrate hexahydrate (>99.0%), NaOH (>98%), and HCl (37%) that were purchased. Shanghai Chemical Industrial Company (Shanghai, China) was the supplier of urea (≥99.0%) and methylene blue (>98%). Before any experiments, fresh solutions were made using distilled water.

3.2. Synthesis of CuAl-LDH and MnAl-LDH

CuAl-LDHs were produced utilizing the technique mentioned earlier with little modifications [54]. Usually, hot water was used to dissolve copper and aluminum nitrates. Urea was added to the dissolved material to form a clear solution. This mixture was then transferred to a round-bottom flask, and deionized water was added to increase the volume to 400 mL. Copper nitrate, aluminum nitrate, and urea were maintained in a molar ratio of 2:1:10. The mixture was continuously stirred for 48 h at 95 °C. After this period, white precipitates formed. These precipitates were separated from the solution using pressure filtration and then dried for ten hours at 70 °C in a traditional drying oven (Figure 9). Using the same process as previously described, manganese nitrate was used in place of copper nitrate to create MnAl-LDH.

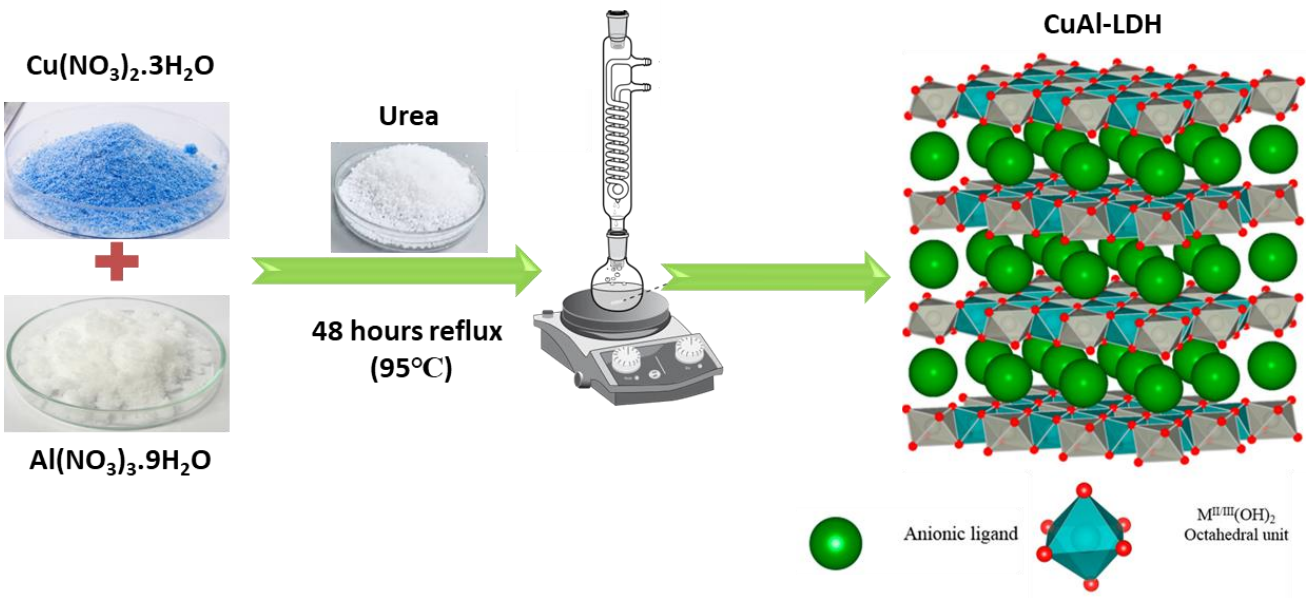

Figure 9. Graphical demonstration of fabrication of CuAl-LDH by hydrothermal method.

3.3. Photocatalytic Degradation Experiments

To test the composite's adsorption effectiveness, 20 mg of the LDH catalyst was added to 20 mL of the 20 mg/L MB solution, and the mixture was swirled in the dark. Portions of 5 mL were taken out of the reaction mixture at predetermined intervals and centrifuged to extract the photocatalysts. Using a spectrophotometer, the methylene blue solutions were measured at 665 nm [42]. Numerous experimental parameters were examined and optimized, including contact time (0–180 min), initial MB concentration (05, 10, 15, 20 and 25 mg/L), and initial pH (4, 6.5, 9).

The following formula has been used to calculate the MB's deterioration rate:

$$D = \frac{C_0 - C_t}{C_0} \times 100\% \quad (7)$$

where C_t is the final concentration of MB and C_0 is its initial concentration. Similar reaction conditions were also used in blank experiments conducted without a catalyst. To determine the ideal conditions for the degradation process, the impacts of different reaction parameters, including the amount of catalyst, the concentration of MB, and pH, were also investigated. All experiments were carried out in duplicate to guarantee accuracy.

4. Conclusions

CuAl-LDH and MnAl-LDH were effectively synthesized using a hydrothermal method, and they were then employed for an improved photocatalytic breakdown of methylene blue when exposed to visible light. The CuAl-LDH and MnAl-LDH nanosheets' XRD and SEM analysis verified the existence of the peak of brucite-like LDH structural features. The photodegradation of MB through the use of CuAl-LDH and MnAl-LDH nanosheets is influenced by several factors, such as pH, catalyst dose, and different concentrations of MB. The CuAl-LDH and MnAl-LDH nanosheets attained 74.95 and 70.93% MB degradation at 180 min under ideal operating conditions. Moreover, both LDH materials showed an excellent performance at up to four cycles, proving its chemical stability and wise use as an environmentally friendly photocatalyst. In a basic environment with visible light, the produced LDH nanosheets exhibit a significant photocatalytic activity that is comparable to previously reported materials. CuAl-LDH and MnAl-LDH nanosheets have a great ability to remove MB from wastewater, as demonstrated by the suggested results, and can be a good candidate for the treatment of industrial wastewater.

Author Contributions: M.A.N. performed the experiments and prepared the original draft. A.u.R., T.N. and M.F.E. performed the data curation, data validation and editing and revision of the draft. M.A.A. and I.H. contributed to manuscript preparation, spectroscopic analysis, visualization, and data interpretation. S.S.A.S. and M.K.T. conceptualized the idea, provided resources, managed the project, and supervised the research. All authors have read and agreed to the published version of the manuscript.

Funding: This research was funded by researchers supporting project number (RSP2024R306), King Saud University, Riyadh, Saudi Arabia.

Data Availability Statement: Data are contained within the article.

Acknowledgments: The authors are thankful to the Institute of Chemistry, The Islamia University of Bahawalpur, for providing a platform to complete this research project. The authors also extend their appreciation to the researchers supporting project number (RSP2024R306), King Saud University, Riyadh, Saudi Arabia. The research funding from the Ministry of Science and Higher Education of the Russian Federation (Ural Federal University Program of Development within the Priority-2030 Program) is also gratefully acknowledged.

Conflicts of Interest: The authors declare no conflicts of interest.

References

1. Nazir, M.A.; Yasar, A.; Bashir, M.A.; Siyal, S.H.; Najam, T.; Javed, M.S.; Ahmad, K.; Hussain, S.; Anjum, S.; Hussain, E.; et al. Quality assessment of the noncarbonated-bottled drinking water: Comparison of their treatment techniques. *Int. J. Environ. Anal. Chem.* **2022**, *102*, 8195–8206. [CrossRef]
2. Bobde, P.; Sharma, A.K.; Panchal, D.; Patel, R.K.; Dhodapkar, R.S.; Pal, S. Layered double hydroxides (LDHs)-based photocatalysts for dye degradation: A review. *Int. J. Environ. Sci. Technol.* **2023**, *20*, 5733–5752. [CrossRef]
3. Sun, H.; Lee, S.-Y.; Park, S.-J. MgAl-layered double hydroxides decorated with Pd-doped SnS nanoparticles: A novel photocatalyst for efficient dye degradation and Cr(VI) reduction in water. *J. Ind. Eng. Chem.* **2023**, *126*, 510–519. [CrossRef]
4. Kumar, O.P.; Nazir, M.A.; Shah, S.S.A.; Hashem, A.; Kumar, A.; Abd_Allah, E.F.; ur Rehman, A. Ternary metal conjugated ZIF-67 coordination with Ag and Ce for the efficient Fenton-like remediation of dyes under visible light. *Opt. Mater.* **2024**, *150*, 115228. [CrossRef]
5. Ishfaq, M.; Khan, S.A.; Nazir, M.A.; Ali, S.; Younas, M.; Mansha, M.; Shah, S.S.A.; Arshad, M.; ur Rehman, A. The in situ synthesis of sunlight-driven Chitosan/MnO_2@MOF-801 nanocomposites for photocatalytic reduction of Rhodamine-B. *J. Mol. Struct.* **2024**, *1301*, 137384. [CrossRef]
6. Sun, L.; Mo, Y.; Zhang, L. A mini review on bio-electrochemical systems for the treatment of azo dye wastewater: State-of-the-art and future prospects. *Chemosphere* **2022**, *294*, 133801. [CrossRef] [PubMed]

7. Pang, Y.L.; Abdullah, A.Z.; Bhatia, S. Review on sonochemical methods in the presence of catalysts and chemical additives for treatment of organic pollutants in wastewater. *Desalination* **2011**, *277*, 1–14. [CrossRef]
8. Han, T.H.; Khan, M.M.; Kalathil, S.; Lee, J.; Cho, M.H. Simultaneous Enhancement of Methylene Blue Degradation and Power Generation in a Microbial Fuel Cell by Gold Nanoparticles. *Ind. Eng. Chem. Res.* **2013**, *52*, 8174–8181. [CrossRef]
9. Yusuf, L.A.; Ertekin, Z.; Fletcher, S.; Symes, M.D. Enhanced ultrasonic degradation of methylene blue using a catalyst-free dual-frequency treatment. *Ultrason. Sonochem.* **2024**, *103*, 106792. [CrossRef] [PubMed]
10. Nazir, M.A.; Najam, T.; Shahzad, K.; Wattoo, M.A.; Hussain, T.; Tufail, M.K.; Shah, S.S.A.; ur Rehman, A. Heterointerface engineering of water stable ZIF-8@ZIF-67: Adsorption of rhodamine B from water. *Surf. Interfaces* **2022**, *34*, 102324. [CrossRef]
11. Anum, A.; Nazir, M.A.; Ibrahim, S.M.; Shah, S.S.A.; Tahir, A.A.; Malik, M.; Wattoo, M.A.; ur Rehman, A. Synthesis of Bi-Metallic-Sulphides/MOF-5@ graphene Oxide Nanocomposites for the Removal of Hazardous Moxifloxacin. *Catalysts* **2023**, *13*, 984. [CrossRef]
12. Cerqueira, A.; Russo, C.; Marques, M. Electroflocculation for textile wastewater treatment. *Braz. J. Chem. Eng.* **2009**, *26*, 659–668. [CrossRef]
13. Ullah, S.; ur Rehman, A.; Najam, T.; Hossain, I.; Anjum, S.; Ali, R.; Shahid, M.U.; Shah, S.S.A.; Nazir, M.A. Advances in metal-organic framework@activated carbon (MOF@AC) composite materials: Synthesis, characteristics and applications. *J. Ind. Eng. Chem.* 2024; *in press*. [CrossRef]
14. Anum, A.; Ibrahim, S.M.; Tahir, A.A.; Nazir, M.A.; Malik, M.; Shah, S.S.A.; Ehsan, A.; Wattoo, M.A.; ur Rehman, A. Construction of hybrid sulfur-doped MOF-235@g-C3N4 photocatalyst for the efficient removal of nicotine. *Inorg. Chem. Commun.* **2023**, *157*, 111268. [CrossRef]
15. Malik, M.; Ibrahim, S.M.; Tahir, A.A.; Nazir, M.A.; Shah, S.S.A.; Wattoo, M.A.; Kousar, R.; ur Rehman, A. Novel approach towards ternary magnetic g-C_3N_4/ZnO-W/Snx nanocomposite: Photodegradation of nicotine under visible light irradiation. *Int. J. Environ. Anal. Chem.* **2023**, 1–19. [CrossRef]
16. Nazir, M.A.; Javed, M.S.; Islam, M.; Assiri, M.A.; Hassan, A.M.; Jamshaid, M.; Najam, T.; Shah, S.S.A.; ur Rehman, A. MOF@graphene nanocomposites for energy and environment applications. *Compos. Commun.* **2024**, *45*, 101783. [CrossRef]
17. Shahzad, K.; Khan, M.I.; Shanableh, A.; Elboughdiri, N.; Jabeen, S.; Nazir, M.A.; Farooq, N.; Ali, H.; Abdelfattah, A.; Rehman, A.U. Silver supported-Ag@PMOS onto thumb structured porous organosilica materials with efficient hetero-junction active sites for photo-degradation of methyl orange dye. *Inorg. Nano-Met. Chem.* **2021**, *52*, 407–416. [CrossRef]
18. Jamshaid, M.; Khan, H.; Nazir, M.A.; Wattoo, M.A.; Shahzad, K.; Malik, M.; Rehman, A.-U. A novel bentonite–cobalt doped bismuth ferrite nanoparticles with boosted visible light induced photodegradation of methyl orange: Synthesis, characterization and analysis of physiochemical changes. *Int. J. Environ. Anal. Chem.* **2022**, *104*, 1186–1201. [CrossRef]
19. Ullah, S.; Shah, S.S.A.; Altaf, M.; Hossain, I.; El Sayed, M.E.; Kallel, M.; El-Bahy, Z.M.; ur Rehman, A.; Najam, T.; Nazir, M.A. Activated carbon derived from biomass for wastewater treatment: Synthesis, application and future challenges. *J. Anal. Appl. Pyrolysis* **2024**, *179*, 106480. [CrossRef]
20. Tian, D.; Zhou, H.; Zhang, H.; Zhou, P.; You, J.; Yao, G.; Pan, Z.; Liu, Y.; Lai, B. Heterogeneous photocatalyst-driven persulfate activation process under visible light irradiation: From basic catalyst design principles to novel enhancement strategies. *Chem. Eng. J.* **2022**, *428*, 131166. [CrossRef]
21. Tonda, S.; Jo, W.-K. Plasmonic Ag nanoparticles decorated NiAl-layered double hydroxide/graphitic carbon nitride nanocomposites for efficient visible-light-driven photocatalytic removal of aqueous organic pollutants. *Catal. Today* **2018**, *315*, 213–222. [CrossRef]
22. Akbarzadeh, A.; Khazani, Y.; Khaloo, S.S.; Ghalkhani, M. Highly effectual photocatalytic degradation of tartrazine by using Ag nanoparticles decorated on Zn-Cu-Cr layered double hydroxide@ 2D graphitic carbon nitride (C_3N_5). *Environ. Sci. Pollut. Res.* **2023**, *30*, 12903–12915. [CrossRef] [PubMed]
23. Nazir, M.A.; Najam, T.; Jabeen, S.; Wattoo, M.A.; Bashir, M.S.; Shah, S.S.A.; ur Rehman, A. Facile synthesis of Tri-metallic layered double hydroxides (NiZnAl-LDHs): Adsorption of Rhodamine-B and methyl orange from water. *Inorg. Chem. Commun.* **2022**, *145*, 110008. [CrossRef]
24. Najam, T.; Aslam, M.K.; Rafiq, K.; Altaf Nazir, M.; Rehman, A.u.; Imran, M.; Javed, M.S.; Cai, X.; Shah, S.S.A. Nanostructure engineering by surficial induced approach: Porous metal oxide-carbon nanotube composite for lithium-ion battery. *Mater. Sci. Eng. B* **2021**, *273*, 115417. [CrossRef]
25. Zhang, X.; Zhang, J.; Qiu, L.; Lan, X.; Zhu, C.; Duan, J.; Liu, Y.; Li, H.; Yu, Y.; Yang, W. In-situ synthesis of dual Z-scheme heterojunctions of cuprous oxide/layered double hydroxides/nitrogen-rich graphitic carbon nitride for photocatalytic sterilization. *J. Colloid Interface Sci.* **2022**, *620*, 313–321. [CrossRef]
26. Jin, Z.-L.; Wang, Y.-P. Strategy of Graphdiyne ($g-C_nH_{2n-2}$) Preparation Coupling with the Flower-Like NiAl-LDH Heterojunctions for Efficient Photocatalytic Hydrogen Evolution. *Chem. Eur. J.* **2021**, *27*, 12649–12658. [CrossRef] [PubMed]
27. Zhang, S.; Zhao, Y.; Shi, R.; Zhou, C.; Waterhouse, G.I.N.; Wu, L.-Z.; Tung, C.-H.; Zhang, T. Efficient Photocatalytic Nitrogen Fixation over Cuδ+-Modified Defective ZnAl-Layered Double Hydroxide Nanosheets. *Adv. Energy Mater.* **2020**, *10*, 1901973. [CrossRef]
28. Karim, A.V.; Hassani, A.; Eghbali, P.; Nidheesh, P. Nanostructured modified layered double hydroxides (LDHs)-based catalysts: A review on synthesis, characterization, and applications in water remediation by advanced oxidation processes. *Curr. Opin. Solid State Mater. Sci.* **2022**, *26*, 100965. [CrossRef]

29. Coogan, Á.; Doménech, N.G.; Mc Ginley, D.; Simonian, T.; Rafferty, A.; Fedix, Q.; Donlon, A.; Nicolosi, V.; Gun'ko, Y.K. Layered double hydroxide/boron nitride nanocomposite membranes for efficient separation and photodegradation of water-soluble dyes. *J. Mater. Chem. A* **2023**, *11*, 12266–12281. [CrossRef]
30. Nazir, M.A.; Khan, N.A.; Cheng, C.; Shah, S.S.A.; Najam, T.; Arshad, M.; Sharif, A.; Akhtar, S.; ur Rehman, A. Surface induced growth of ZIF-67 at Co-layered double hydroxide: Removal of methylene blue and methyl orange from water. *Appl. Clay Sci.* **2020**, *190*, 105564. [CrossRef]
31. Nazir, M.A.; Bashir, M.A.; Najam, T.; Javed, M.S.; Suleman, S.; Hussain, S.; Kumar, O.P.; Shah, S.S.A.; ur Rehman, A. Combining structurally ordered intermetallic nodes: Kinetic and isothermal studies for removal of malachite green and methyl orange with mechanistic aspects. *Microchem. J.* **2021**, *164*, 105973. [CrossRef]
32. Hanifah, Y.; Mohadi, R.; Lesbani, A. Polyoxometalate Intercalated MgAl-Layered Double Hydroxide for Degradation of Malachite Green. *Ecol. Eng. Environ. Technol.* **2023**, *24*, 109–119. [CrossRef]
33. Bharali, D.; Saikia, S.; Devi, R.; Choudary, B.M.; Gour, N.K.; Deka, R.C. Photocatalytic degradation of phenol and its derivatives over ZnFe layered double hydroxide. *J. Photochem. Photobiol. A Chem.* **2023**, *438*, 114509. [CrossRef]
34. Zhang, C.; Liang, X.; Lu, Y.; Li, H.; Xu, X. Performance of CuAl-LDH/Gr Nanocomposite-Based Electrochemical Sensor with Regard to Trace Glyphosate Detection in Water. *Sensors* **2020**, *20*, 4146. [CrossRef] [PubMed]
35. Lu, Y.; Liang, X.; Xu, J.; Zhao, Z.; Tian, G. Synthesis of $CuZrO_3$ nanocomposites/graphene and their application in modified electrodes for the co-detection of trace Pb (II) and Cd (II). *Sens. Actuators B Chem.* **2018**, *273*, 1146–1155. [CrossRef]
36. Berner, S.; Araya, P.; Govan, J.; Palza, H. Cu/Al and Cu/Cr based layered double hydroxide nanoparticles as adsorption materials for water treatment. *J. Ind. Eng. Chem.* **2018**, *59*, 134–140. [CrossRef]
37. Akhter, P.; Nawaz, S.; Shafiq, I.; Nazir, A.; Shafique, S.; Jamil, F.; Park, Y.-K.; Hussain, M. Efficient visible light assisted photocatalysis using ZnO/TiO_2 nanocomposites. *Mol. Catal.* **2023**, *535*, 112896. [CrossRef]
38. Nayak, S.; Kumar Das, K.; Parida, K. Indulgent of the physiochemical features of MgCr-LDH nanosheets towards photodegradation process of methylene blue. *J. Colloid Interface Sci.* **2023**, *634*, 121–137. [CrossRef] [PubMed]
39. Jin, L.; Zeng, H.-Y.; Xu, S.; Chen, C.-R.; Duan, H.-Z.; Du, J.-Z.; Hu, G.; Sun, Y.-X. Facile preparation of sepiolite@LDH composites for the visible-light degradation of organic dyes. *Chin. J. Catal.* **2018**, *39*, 1832–1841. [CrossRef]
40. Wang, Z.; Wang, X.; Wang, L.; Wei, Y.; Zhao, Z.; Du, K.; Chen, D.; Li, X.; Zhou, C.; Liu, G. ZIF-67-derived Co@ N-PC anchored on tracheid skeleton from sawdust with micro/nano composite structures for boosted methylene blue degradation. *Sep. Purif. Technol.* **2021**, *278*, 119489. [CrossRef]
41. Jamshaid, M.; Nazir, M.A.; Najam, T.; Shah, S.S.A.; Khan, H.M.; ur Rehman, A. Facile synthesis of Yb^{3+}-Zn^{2+} substituted M type hexaferrites: Structural, electric and photocatalytic properties under visible light for methylene blue removal. *Chem. Phys. Lett.* **2022**, *805*, 139939. [CrossRef]
42. Malik, M.; Ibrahim, S.M.; Nazir, M.A.; Tahir, A.A.; Tufail, M.K.; Shah, S.S.A.; Anum, A.; Wattoo, M.A.; ur Rehman, A. Engineering of a Hybrid g-C_3N_4/ZnO-W/Co_x Heterojunction Photocatalyst for the Removal of Methylene Blue Dye. *Catalysts* **2023**, *13*, 813. [CrossRef]
43. Shahzad, K.; Najam, T.; Bashir, M.S.; Nazir, M.A.; ur Rehman, A.; Bashir, M.A.; Shah, S.S.A. Fabrication of Periodic Mesoporous Organo Silicate (PMOS) composites of Ag and ZnO: Photo-catalytic degradation of methylene blue and methyl orange. *Inorg. Chem. Commun.* **2021**, *123*, 108357. [CrossRef]
44. Shahzad, K.; Hussain, S.; Nazir, M.A.; Jamshaid, M.; ur Rehman, A.; Alkorbi, A.S.; Alsaiari, R.; Alhemiary, N.A. Versatile Ag_2O and ZnO nanomaterials fabricated via annealed Ag-PMOS and ZnO-PMOS: An efficient photocatalysis tool for azo dyes. *J. Mol. Liq.* **2022**, *356*, 119036. [CrossRef]
45. Wang, X.; Hu, J.; Guan, H.; Dai, X.; Wu, M.; Wang, X. Wood-based catalytic filter decorated with ZIF-67 for highly efficient and continuous organic pollutant removal. *Chem. Eng. J.* **2024**, *479*, 147580. [CrossRef]
46. Li, Y.; Wang, Y.; Liu, L.; Tian, L. Non-radical-dominated catalytic degradation of methylene blue by magnetic $CoMoO_4/CoFe_2O_4$ composite peroxymonosulfate activators. *J. Environ. Manag.* **2023**, *325*, 116587. [CrossRef] [PubMed]
47. Şendal, K.; Üstün Özgür, M.; Gülen, J. Biosynthesis of ZnO photocatalyst and its application in photo catalytic degradation of methylene blue dyestuff. *J. Dispers. Sci. Technol.* **2023**, *44*, 2734–2747. [CrossRef]
48. Chen, L.; Ou, S.-F.; Nguyen, T.-B.; Chuang, Y.; Chen, C.-W.; Dong, C.-D. In-situ hydrothermal synthesis of MoS_2/TiO_2 nanocomposites for enhanced and stable photocatalytic performance: Methylene blue degradation pathway and mechanism. *J. Taiwan Inst. Chem. Eng.* **2024**, 105436. [CrossRef]
49. Vicencio Garrido, M.A.; Chávez Portillo, M.; Juarez, H.; Luna, A.; Serrano-De la Rosa, L.E. Low cost chemical bath deposition synthesis of Zinc Oxide/Zinc sulfide composite and Zinc hydrozincite for methylene blue degradation. *Inorg. Chem. Commun.* **2024**, *164*, 112484. [CrossRef]
50. Akhter, P.; Ali, F.; Ali, A.; Hussain, M. TiO_2 decorated CNTs nanocomposite for efficient photocatalytic degradation of methylene blue. *Diam. Relat. Mater.* **2024**, *141*, 110702. [CrossRef]
51. Boumeriame, H.; Cherevan, A.; Eder, D.; Apaydin, D.H.; Chafik, T.; Da Silva, E.S.; Faria, J.L. Engineering g-C_3N_4 with CuAl-layered double hydroxide in 2D/2D heterostructures for visible-light water splitting. *J. Colloid Interface Sci.* **2023**, *652*, 2147–2158. [CrossRef] [PubMed]
52. Woo, M.A.; Kim, T.W.; Kim, I.Y.; Hwang, S.-J. Synthesis and lithium electrode application of $ZnO-ZnFe_2O_4$ nanocomposites and porously assembled $ZnFe_2O_4$ nanoparticles. *Solid State Ion.* **2011**, *182*, 91–97. [CrossRef]

53. Xia, S.; Zhang, L.; Pan, G.; Qian, P.; Ni, Z. Photocatalytic degradation of methylene blue with a nanocomposite system: Synthesis, photocatalysis and degradation pathways. *Phys. Chem. Chem. Phys.* **2015**, *17*, 5345–5351. [CrossRef] [PubMed]
54. Nazir, M.A.; Najam, T.; Bashir, M.S.; Javed, M.S.; Bashir, M.A.; Imran, M.; Azhar, U.; Shah, S.S.A.; ur Rehman, A. Kinetics, isothermal and mechanistic insight into the adsorption of eosin yellow and malachite green from water via tri-metallic layered double hydroxide nanosheets. *Korean J. Chem. Eng.* **2022**, *39*, 216–226. [CrossRef]

Disclaimer/Publisher's Note: The statements, opinions and data contained in all publications are solely those of the individual author(s) and contributor(s) and not of MDPI and/or the editor(s). MDPI and/or the editor(s) disclaim responsibility for any injury to people or property resulting from any ideas, methods, instructions or products referred to in the content.